

# Erosive Burning

J. P. Renie\* and J. R. Osborn†  
Purdue University, West Lafayette, Indiana

A new and unique mathematical model is presented for determining the erosive burning rate of a composite solid propellant. This model is based on the hypothesis of Corner and Lengelle that the erosive burning effect is due to an increase in the value of the transport properties in the gas-phase reaction zone caused by the presence of a turbulent boundary layer. This model couples a unique statistical combustion model, the petite ensemble model (PEM), with an approximate boundary-layer analysis for flow over a transpiring surface so that the effects of cross-flow velocity, base burning rate, pressure, and surface roughness on the erosive burning sensitivity of a composite solid propellant can be predicted. Theoretical results indicate that erosive burning sensitivity is directly related to the characteristics of the blown boundary layer within the gas-phase reaction zone directly above the propellant surface.

## Nomenclature

$b$	= blowing parameter, defined by Eq. (8)
$C_{f0}$	= zero-blowing skin friction coefficient, defined by Eq. (9)
$DF$	= damping factor in Prandtl mixing length expression, Eq. (4)
$D_h$	= duct hydraulic diameter
$D_{ox}$	= oxidizer particle diameter
$F_d$	= oxidizer distribution function
$k_s$	= average surface roughness height
$K$	= constant in Prandtl mixing length expression, Eq. (4)
$\ell_m$	= Prandtl mixing length, defined by Eq. (4)
$m_T$	= planar surface mass flux
$r_d$	= pseudopropellant linear burning rate
$r_T$	= linear propellant burning rate
$Re$	= Reynolds number based on duct hydraulic diameter
$u_g$	= local cross-stream velocity component
$U_\infty$	= freestream cross-flow velocity
$x$	= cross-stream coordinate
$y$	= surface-normal coordinate
$\Delta y$	= boundary-layer displacement factor
$y^*$	= variable of integration in Eq. (11)
$\hat{y}$	= transformed surface-normal coordinate
$\alpha_d$	= pseudopropellant oxidizer mass fraction
$\beta$	= local transport enhancement factor
$\beta_{av}$	= average transport enhancement factor, defined by Eq. (11)
$\epsilon_g$	= eddy diffusivity of momentum of gas phase
$\phi$	= cross-stream velocity gradient, $du_g/d\hat{y}$
$\mu_g$	= molecular viscosity of gas phase
$\rho_g$	= density of gas phase
$\rho_s$	= density of propellant solid phase
$\tau_w$	= blowing wall shear stress
$\tau_{w0}$	= zero-blowing wall shear stress

## Introduction

**R**EQUIREMENTS for ever higher propellant loading in solid-propellant rocket motors have led to the

Presented as Paper 79-0165 at the AIAA 17th Aerospace Sciences Meeting, New Orleans, La., Jan. 15-17, 1979; submitted Feb. 12, 1979; revision received June 7, 1982. Copyright © American Institute of Aeronautics and Astronautics, Inc., 1983. All rights reserved.

\*Graduate Student, School of Aeronautics and Astronautics. Student Member AIAA.

†Professor, School of Aeronautics and Astronautics. Associate Fellow AIAA.

development of grain configurations with relatively low port-to-throat area ratios. This, in turn, results in high velocities of the propellant combustion gases flowing across the burning propellant surfaces in the aft region of the propellant grains. The presence of a high cross-flow velocity over a propellant burning surface causes enhancement of the propellant burning rate and this enhancement of burning rate is termed erosive burning. For high cross-flow velocities, the burning rate can be substantially higher than the burning rate of the same propellant not subject to a cross-flow velocity. Moreover, the effects of erosive burning are critical in that the erosive burning rate contributions strongly influence performance level and performance repeatability of propulsion systems.

Since erosive burning is present in many solid-propellant propulsion systems and since there is such a strong interaction between the local flow environment and the propellant burning rate, it is necessary to be able to predict this interaction in order to design and calculate the performance of a low port-to-throat area ratio rocket. This paper presents a model that can be used to predict propellant burning rate behavior under erosive conditions.

## Background

A number of erosive burning models have appeared in the literature, along with several critical reviews of the erosive burning literature; the two most recently being those of Kuo and Razdan<sup>1</sup> and King.<sup>2</sup> In his review, King classifies the models into several categories, including:

1) Models based on the heat transfer from a "core" gas to the propellant surface by forced convection.

2) Models based on the alteration of transport properties in the gas-phase reaction zone by cross-flow induced turbulence.

3) Models based on chemically reacting boundary-layer theory.

In that review King demonstrated quite clearly that models of the first category do not correctly predict the experimental data. That is, the experimental erosion rate is independent of the driver gas stagnation temperature. Therefore, it may be concluded that such models do not accurately describe the erosive burning behavior of a solid propellant.

The other two categories of models are somewhat similar in their approach to the problem. They differ only in the degree to which the fluid mechanics and combustion processes involved have been addressed. On the one hand, in the models of category 2, the boundary layer is treated in an approximate fashion, while the combustion process is treated completely.

On the other hand, with the models of category 3, a complete mathematical solution of the reacting boundary layer is performed while the combustion process is treated as a one-step chemical reaction. Both methods involve the computation of a velocity profile above the propellant surface, and each determines the influence of the profile on the burning rate of the solid propellant. It is to be expected, then, that the superior fluid mechanical model will yield detailed information about the fluid mechanics of the problem, while producing little or no information regarding the effect of propellant parameters on the erosive burning rate. As a result, only those erosive burning models having a combustion model reasonably descriptive of the combustion processes occurring can be expected to provide information useful for the selection of composite propellants for reducing or eliminating erosive burning effects.

One of the more comprehensive studies of erosive burning of the category 3 type is the model suggested by Beddini.<sup>3</sup> In the theoretical study of injection-induced flows in porous walled ducts, Beddini employed a second-order closure model of turbulence, coupled with a single-step reaction to model the combustion/flow interaction within solid-propellant motor cavities. Results indicate that flow from the head end of a solid-propellant rocket motor to the nozzle entrance can undergo three regimes of development. In the first regime, the velocity field develops in accordance with laminar similarity theory. High levels of turbulence build up in the second regime, leading to a transition of the mean axial velocity profile. The third regime, or fully turbulent flow, occurs at large Reynolds numbers and corresponds to conditions within rocket motors for which erosive burning is present, that is, for high cross-flow velocities near the port end of the grain. Beddini found that the character of the flow within the third regime is predicted to be similar in some respects to wall-bounded turbulent shear flow with surface injection. In particular, the initiation of erosive burning is consistently found to be preceded by transition of the mean axial velocity profile within the grain port—the point of transition being directly related to the motor scaling. Finally, Beddini's predictions correspond with the classical and conventional concept that erosive burning is due to enhanced turbulent thermal diffusion within the coexistent viscous sublayer/combustion zone.

In this paper, an erosive burning model of the category 2 type then employs a statistical, steady-state combustion model, the petite ensemble model (PEM),<sup>4,5</sup> is described and subsequent erosive burning calculations are presented. Confirmed by the extensive fluid mechanical calculations of Beddini which indicate that erosive burning occurs only in the region of the motor grain for which fully developed turbulent flow exists, an approximate turbulent boundary-layer analysis is employed for computing the velocity profile about a transpiring propellant surface. In this model, it is hypothesized that the erosive burning effect is due to an enhancement of the transport properties of thermal conductivity and mass diffusivity in the region of the gas-phase reaction zone as suggested by Corner<sup>6</sup> and Lengelle.<sup>7</sup> An earlier version of this approximate analysis of the turbulent boundary layer above a flat surface is described in more detail in Renie and Osborn.<sup>5,8</sup> This analysis is an improvement over an original method employed by Condon and Osborn<sup>4,9</sup> and will subsequently be referred to as the PEM approximate analysis, or the erosive PEM method. This method is similar to the momentum integral analysis employed currently in the erosive burning modeling efforts of King.<sup>10</sup> The boundary-layer profile characteristics and subsequent transport property enhancement are shown to be strongly dependent on cross-flow velocity, propellant burning rate, pressure, and surface roughness. These results will be presented along with the prediction of actual experimental erosive burning data obtained for a series of composite solid propellants.

### Composite Propellant Combustion Model

The PEM is a steady-state combustion model that combines a statistical formalism<sup>11</sup> and a combustion model similar in several respects to the Beckstead, Derr, and Price (BDP) model.<sup>12</sup> In the PEM, the burning surface is treated as a fuel plane dotted with protruding and/or recessed oxidizer surfaces. The number and dimensions of these surfaces are dependent on both propellant formulation variables and combustion parameters. Furthermore, it is assumed that the flames associated with a given oxidizer particle do not interact with the flames of surrounding oxidizer particles. With these assumptions, the burning surface of polydisperse propellants (distribution of oxidizer diameters) can be rearranged into imaginary families of monodisperse (only one oxidizer diameter) propellants called pseudopropellants. A further assumption employed with this description is that each oxidizer particle at the burning surface has associated with it some portion of the available fuel.

The mass flux from the entire polydisperse propellant surface and, consequently, its mean linear burning rate can then be determined by a statistical summation process over all oxidizer diameters of the monodisperse, pseudopropellant mass fluxes. The mathematical expression for the total propellant burning rate, can be written in the following form:

$$r_T = \int_{D_{ox}} \frac{r_d}{\alpha_d} F_d d\ln D_{ox} \quad (1)$$

The reader is referred to Refs. 4, 5, 13, and 14 for a more complete description of the statistically based burning rate expression given above.

In this manner, the total propellant burning rate is expressed in terms of propellant formulation variables and the monodisperse pseudopropellant burning rates. The propellant formulation variables are selected in the form of the oxidizer particle size and size distribution, the oxidizer mass fraction, and other oxidizer/binder characteristics. The monodisperse pseudopropellant burning rates are determined from the unit flame combustion model fully described in Refs. 4 and 5. The integration over all oxidizer particle sizes for the burning rate of a polydisperse propellant, that is, Eq. (1), forms the petite ensemble model (PEM).

The PEM briefly described above thus permits consideration of a real propellant having an oxidizer particle size distribution. This model represents a significant improvement over the early conventional models which require that a single particle size be selected to represent the polydispersion of oxidizer particle sizes present in all real propellants.

### PEM Approximate Boundary-Layer Analysis

In the erosive burning model described in Renie and Osborn,<sup>5,8</sup> the turbulent boundary layer above the propellant surface is modeled by an approximate solution of the conservation of mass equation and the Navier-Stokes equation representing the conservation of momentum for the flow over a flat surface with surface-normal mass injection. These equations are applied to turbulent flow by representing each of the dependent flow properties as the sum of a time-averaged quantity and an instantaneous quantity. The resulting equations are then time averaged and the usual boundary-layer assumptions are imposed.<sup>15</sup> For the present analysis, it is assumed that the fluid properties of viscosity and density remain constant throughout the flowfield. It is also assumed that the variations of the dependent flow properties with respect to the cross-stream coordinate  $x$  are negligible compared to their variations with respect to the surface-normal coordinate  $y$ .

By integrating the conservation of mass equation and incorporating the resulting expression along with the Boussinesq relation<sup>16</sup> for the eddy diffusivity of momentum,

the conservation of momentum equation for a turbulent boundary layer situated above a flat surface with uniform surface mass injection can be written

$$m_T \frac{du_g}{dy} = (\mu_g + \rho_g \epsilon_g) \frac{d^2 u_g}{dy^2} + \rho_g \frac{du_g}{dy} \frac{d\epsilon_g}{dy} \quad (2)$$

The planar mass flux is equal to the product of the linear burning rate given by Eq. (1) and the solid-propellant density. Equation (2) will be used to determine the boundary layer above a transpiring flat surface within a confined channel. Due to the effects of friction and mass addition for flow through a duct, an axial pressure term may not be negligible and should be incorporated within the momentum equation above. King<sup>10</sup> has included such an axial pressure term within his momentum integral analysis. However, both King and the authors have found that this term is negligible except for conditions corresponding to large surface blowing, where the velocity profile is calculated as being blown away from the surface to such an extent that the erosive burning sensitivity is virtually nonexistent.

If it is assumed that the Prandtl mixing length hypothesis<sup>16</sup> is valid for the case of surface mass injection, or blowing, then the eddy diffusivity of momentum can be written

$$\epsilon_g = \ell_m^2 \frac{du_g}{dy} \quad (3)$$

The Prandtl mixing length can be written in the following fashion, modified in such a manner as to account for the combined effects of the proximity of a rough blown wall, or

$$\ell_m = K(y + \Delta y) DF \quad (4)$$

In the above expression,  $K$  is a constant and  $\ell_m$  has been modified from the original concept of the mixing length to represent the influence of surface roughness recognizing the fact that the velocity profiles for smooth and rough walls can be similar, provided that the normal coordinate  $y$  is displaced by an amount  $\Delta y$ . This displacement factor  $\Delta y$  is given as a function of an equivalent sand grain roughness  $k_s$  in the work of Cebeci and Chang.<sup>17</sup> Based upon data given in Ref. 16 for the value of equivalent sand grain roughness  $k_s$ , it is assumed that for a given propellant this roughness height will be equal to the mean oxidizer diameter. Obviously, this parameter is a complex function of the distribution of the propellant surface structure about which little information is known. Due to the lack of actual surface structure data, the above assumption is justified. In Eq. (4), an additional parameter,  $DF$ , has been included based on an empirical relation developed in the work

of Kays and Moffat.<sup>18</sup> This damping factor  $DF$  has been subsequently modified by King<sup>10</sup> in an attempt to account for the combined effects of blowing, axial pressure gradient, and surface roughness using approaches suggested by van Driest<sup>19</sup> and Cebeci and Chang.<sup>17</sup> In the results to be presented later, the best agreement between theory and experiment has been obtained utilizing the Prandtl mixing length expression incorporating only the displacement factor based on surface roughness while assuming a unity damping factor.

The following analysis is valid only for a damping factor equal to one and  $\hat{y}$  has been substituted for the displaced normal coordinate  $y + \Delta y$ . By substituting Eqs. (3) and (4) into Eq. (2) and defining a new variable,  $\phi = du_g/d\hat{y}$ , the following nonlinear, first-order differential equation in  $\phi$  as a function of  $\hat{y}$  can be written:

$$m_T \phi = (\mu_g + \rho_g K^2 \hat{y}^2 \phi) \frac{d\phi}{d\hat{y}} + K^2 \rho_g \phi \left[ 2\hat{y}\phi + \hat{y}^2 \frac{d\phi}{d\hat{y}} \right] \quad (5)$$

Equation (5) can be rewritten in the following manner:

$$\frac{d\phi}{d\hat{y}} = \frac{m_T \phi - 2K^2 \rho_g \hat{y}^2 \phi^2}{(\mu_g + 2K^2 \rho_g \hat{y}^2 \phi)} \quad (6)$$

If the value for the blowing wall shear stress at the propellant surface is known, and since  $\phi = \tau_w/\mu_g$  at the surface, then Eq. (6) can be used to determine the variation of  $\phi$  with height above the propellant surface by means of a fourth-order Runge-Kutta scheme. With this information, the variation in both the cross-stream velocity component and the eddy diffusivity of momentum with the surface-normal coordinate can be determined. This information is utilized to enhance the transport properties in the gas-phase reaction zone situated within the turbulent boundary layer above the propellant surface in a manner described below.

Before Eq. (6) can be solved, however, the value of the blowing wall shear stress must be approximated. A number of investigators<sup>18,20-23</sup> have attempted to relate both theoretically and experimentally the blowing wall stress and the zero-blowing wall stress to the blowing parameter. That is,  $\tau_w/\tau_{w0} = f(b)$ . However, based on the multitude of data<sup>18,20-23</sup> it is quite clear that no one expression of the form  $\tau_w/\tau_{w0} = f(b)$  fits all of the available data. For this study, an approximate exponential fit of the following form is employed:

$$\frac{\tau_w}{\tau_{w0}} = \exp(-0.4023b) \quad (7)$$

Obviously, for large values of  $b$  (greater than about 6) corresponding to large burning rates and small cross-flow velocities, the wall shear stress for a blown boundary layer is substantially reduced from its zero-blowing value. Even though experimental data corresponding to these high blowing values are lacking, it will be shown later that very small values of wall shear stress represent a highly blown velocity profile above the propellant surface, resulting in low turbulence levels or corresponding negligible erosive burning sensitivity within these regions.

In a similar fashion to that of Refs. 18 and 20-23 the blowing parameter is given by

$$b = \frac{m_T U_\infty}{\tau_{w0}} = \frac{\rho_s r_T}{\rho_g U_\infty} \left( \frac{2}{C_{f0}} \right) \quad (8)$$

This expression for the blowing parameter has been written incorporating an expression for the zero-blowing skin friction coefficient of the form

$$C_{f0} = \tau_{w0} / \frac{1}{2} \rho_g U_\infty^2 \quad (9)$$

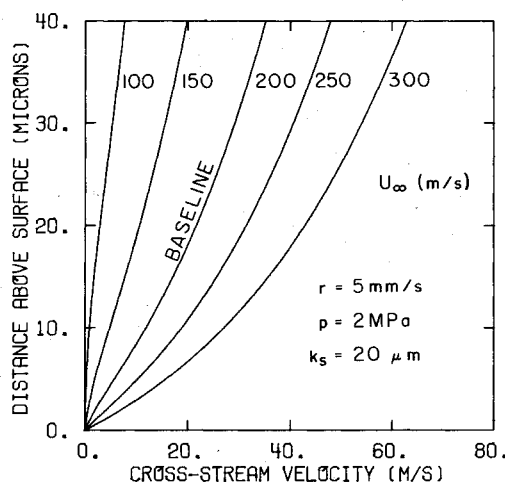


Fig. 1 Velocity profiles.

The zero-blowing skin friction coefficient can be represented by an empirical relation<sup>16</sup> as

$$C_{f0} = \left[ 3.48 - 4 \log_{10} \left( \frac{2k_s}{D_h} + \frac{9.35}{Re} \frac{1}{\sqrt{C_{f0}}} \right) \right]^{-2} \quad (10)$$

With the above information, Eq. (6) can be used to determine the local variation of the turbulent viscosity that is equal to the sum of the molecular and eddy viscosities. It will be shown how this variation in the turbulent viscosity in the vicinity of the propellant surface can be used to determine the enhancement in the transport properties of thermal conductivity and mass diffusivity. It will also be shown that these turbulent transport properties can be coupled to a steady-state combustion model in order to calculate the value of an enhanced burning rate for a propellant subjected to a cross-flow of combustion gases.

### Erosive Burning Model

The PEM-based erosive burning model is based on the hypothesis that the erosive burning effect is due to an enhancement of the transport properties in the region of the gas-phase reaction zone as suggested by Corner<sup>6</sup> and Lengelle.<sup>7</sup> This enhancement is assumed to be due to the presence of a turbulent boundary layer situated above the propellant surface.

In the erosive burning analysis it is assumed that a turbulent boundary layer develops above the propellant surface and that the transport coefficients of thermal conductivity and mass diffusivity are modified in such a manner that the heat flux to the surface and, consequently, the propellant burning rate are enhanced.

It is assumed that in the normal, nonerosive regime, the transport coefficients of thermal conductivity and mass diffusivity are the molecular ones. However, under erosive conditions, the transport coefficients are modified by turbulent components that are dependent upon the nature of the flow. Moreover, in the present analysis, it is assumed that the ratio of the molecular transport property to the total transport property in the presence of turbulence is equal to the ratio of the molecular viscosity to the turbulent viscosity. Since there are three flames of differing heights above the surface considered in the PEM, separate average turbulent transport properties must be calculated for each flame. Thus, there are turbulent thermal conductivities associated with the AP monopropellant flame, the primary flame, and the final diffusion flame, and there are turbulent mass diffusivities associated with the primary flame and the final diffusion flame.

Since the PEM burning rate calculation comprises an iterative solution of several simultaneous equations, a closed-form solution for the erosive burning rate is not possible. Furthermore, the transport properties of thermal conductivity and mass diffusivity used in the burning rate calculations are functions of the burning rate with a strong coupling between the propellant blowing effect, the burning rate, and the turbulent transport property calculations.

Thus, the solution for the erosive burning rate involves iterating on the transport properties and the burning rate. The iteration steps are:

- 1) Calculate the burning rate using the molecular transport properties associated with each of the flame regions.
- 2) Calculate the velocity and eddy diffusivity profiles within the turbulent boundary layer above the propellant surface using the method described above and the burning rate from step 1.
- 3) Calculate the average transport coefficients from the ratio of turbulent to molecular viscosity for each flame region using the eddy diffusivity profile.
- 4) Calculate a new value of burning rate using the enhanced transport coefficients determined in step 3.

5) Iterate on the value of propellant burning rate until the value of burning rate calculated in step 4 matches the burning rate used in step 2.

The process described above is repeated until the desired burning rate convergence is achieved.

Before proceeding to the comparison of erosive burning PEM predictions with experimental data, it is instructive to present and discuss the characteristics of the boundary layer as calculated via the approximate analysis described in the previous section. Both the velocity and average transport enhancement factor profiles have been calculated for a propellant subjected to various flow conditions. A baseline "computer" propellant is assumed to be comprised of 73% ammonium perchlorate (AP) and 27% HTPB fuel binder. The baseline flow conditions are a cross-flow velocity of 200 m/s, a propellant burning rate of 5 mm/s, and a gas-phase pressure of 2 MPa. Also, it is assumed that the surface roughness associated with this baseline propellant is equal to 20  $\mu$ m. For the purposes of illustrating the effects of cross-flow velocity, burning rate, pressure, and surface roughness on the calculated boundary-layer characteristics, each of these parameters has been perturbed about its baseline value. In the following figures, the line marked "baseline" corresponds to calculations associated with this baseline condition.

The average transport enhancement factor presented in the figures has been calculated as a function of height above the propellant surface in the following fashion. Recalling from the previous discussion that under specified surface blowing and cross-flow conditions, Eq. (6) coupled with the Prandtl mixing length expression [Eqs. (3) and (4)] yields the local variation in the turbulent viscosity. The local transport enhancement factor is equal to the ratio of the turbulent viscosity to the molecular viscosity. The average transport enhancement factor is then calculated in an inverse averaging fashion,<sup>5</sup> or

$$\beta_{av}(y) = \left[ \frac{1}{y} \int_0^y \frac{dy^*}{\beta(y^*)} \right]^{-1} \quad (11)$$

Therefore, for a given region extended to a distance  $y$  above the propellant surface, the transport properties of thermal conductivity and mass diffusivity are enhanced by the value of the average transport enhancement factor given above—thus leading to erosive burning.

Figures 1 and 2 depict the calculated velocity profiles for the cross-flow velocity and burning rate perturbations about the baseline condition, respectively. In Fig. 1, the cross-flow velocity has been varied at 100-300 m/s while the burning rate, pressure, and surface roughness remain fixed at their baseline values. The blowing parameter given by Eq. (8) ranges from a low value of 3.4 for the 300 m/s cross-flow case to 5.1 for the baseline condition, and up to a high value of 9.7 for the 100 m/s cross-flow case. Similarly, in Fig. 2, the burning rate has been varied at 0-10 mm/s while the cross-flow velocity, pressure, and surface roughness remain fixed at their baseline values. For results presented in this figure, the blowing parameter ranges from a zero value for the zero burning rate case up to 10.1 for the 10 mm/s burning rate case.

From these first two figures, it is obvious that an increase in the blowing parameter by either a decrease in the cross-flow velocity or an increase in the surface transpiration velocity, or burning rate, causes the velocity profile to steepen dramatically near the surface. That is, the boundary layer, or turbulence, is more easily blown away from the propellant surface as the ratio of the surface mass flux to the cross-stream mass flux is increased or the blowing parameter is increased. This steepening in the velocity profile with a decreasing cross-flow velocity or an increasing burning rate results in a significant decrease in the level of turbulence close to the propellant surface. Therefore, if erosive burning is

postulated as being caused by an enhancement in the values of the transport properties within the flame zones close to the propellant surface, then these results indicate that erosive burning will be greater for lower values of the blowing parameter, or more precisely, higher cross-flow velocities and/or lower burning rates.

Such results are best manifested with a presentation of the calculated average transport enhancement parameter for both the cross-flow velocity perturbation (Fig. 3) and the burning rate perturbation (Fig. 4). From these results, it is quite evident that for a given distance above the propellant surface, a decrease in the blowing parameter by either an increase in the cross-flow velocity or a decrease in the burning rate will yield a corresponding higher turbulence level leading to a larger transport property enhancement and higher erosive burning sensitivity.

Although the results are not presented graphically, similar calculations have been performed to show the effects of varying both pressure and surface roughness on the velocity and average transport enhancement factor profiles. Decreasing pressure causes an increase in the blowing parameter and a steepening in the velocity profile. This effect is primarily due to the reduction in the gas-phase density with decreased pressure. The same effect is observed with a decrease in the value of surface roughness, brought about by a corresponding reduction in the shear stress at the propellant surface with decreased roughness as given in Eq. (10). Similar to the results shown in Figs. 3 and 4 for the cross-flow velocity and burning rate perturbations, the turbulence level near the propellant surface increases with a decrease in the blowing parameter caused by increases in either pressure or surface roughness. Therefore, erosive burning is expected to be greater for higher pressure and surface roughness.

All of the results presented and discussed above, that is, the effects of cross-flow velocity, burning rate, pressure, and surface roughness on the erosive burning sensitivity of a solid propellant, will also be presented in the next section as the erosive burning PEM is employed to predict experimentally observed trends for a series of composite solid propellants.

### Comparison with Experiment

One of the tests of a theory predicting the erosive burning rate is its ability to predict the trends traditionally observed in erosive burning experimental studies. Three of these observations are:

- 1) Threshold velocities exist. That is, burning rate is not affected until the core gas reaches a certain velocity.
- 2) The value of this threshold velocity for a given propellant is a function of pressure: the higher the pressure, the lower the threshold velocity.

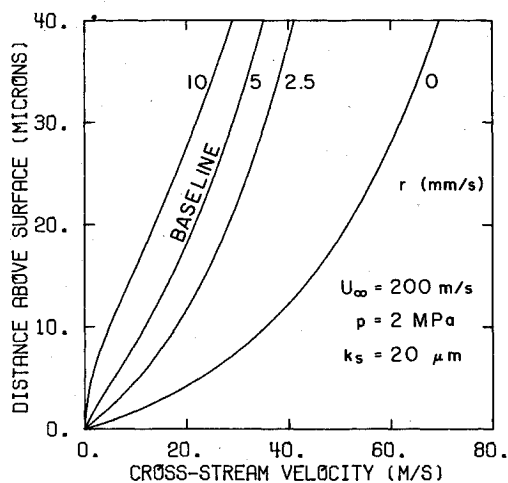


Fig. 2 Velocity profiles.

- 3) Slower burning propellants are more strongly affected by cross flows than higher burning rate formulations.

The above observations have been made primarily in flow systems with cross-flow velocities corresponding to Mach numbers less than 0.3. In this section, it will be shown that the erosive PEM described above correctly predicts these traditionally observed experimental trends. At the same time, both the nonerosive and erosive experimental data of King<sup>10</sup> for a series of composite solid propellants will be presented and compared to the erosive PEM. Finally, in the following section, the erosive PEM will be employed to illustrate the effect of oxidizer particle size on erosive burning sensitivity.

Four of King's<sup>10</sup> composite propellant formulations have been selected for investigation with the erosive PEM. All four formulations are unimodal, AP/HTPB propellants; however, the first three have an identical 73% solids fraction with varying oxidizer particle diameters of 5, 20, and 200  $\mu\text{m}$ . These propellants have been designated as formulation numbers, 4685, 4525, and 5051, respectively. The fourth formulation, No. 5542, is a 77% solid propellant with an oxidizer particle size of 20  $\mu\text{m}$ . Therefore, the erosive burning data for the first three propellant formulations can be used to compare the effect of oxidizer particle size on erosive burning sensitivity. Also, the second and fourth formulations can be used to determine the effects of variations in solids loading on erosive burning. For the latter two propellants, the variation in solids loading will result in both variations in the combustion gas flame temperature and propellant burning rate uncoupled from the oxidizer particle size influences.

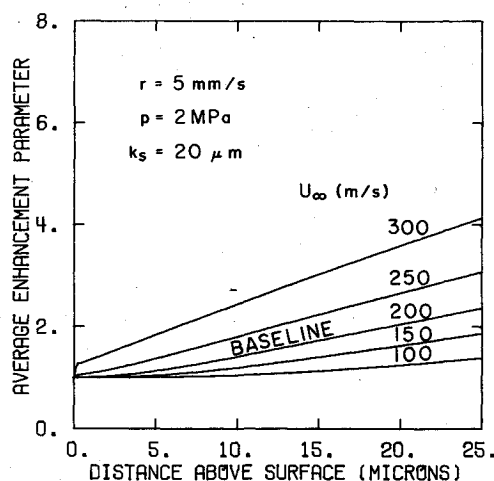


Fig. 3 Enhancement profiles.

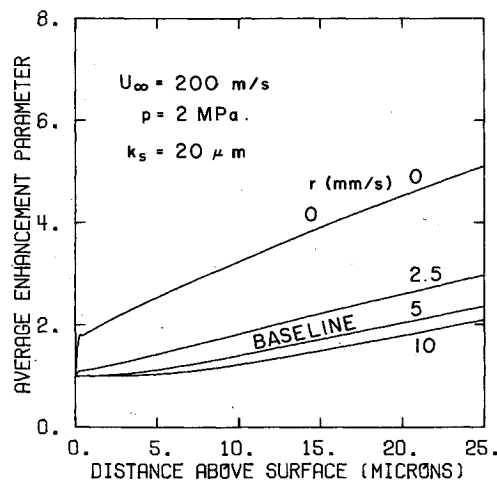


Fig. 4 Enhancement profiles.

Although the experimental data base presented by King<sup>10</sup> is quite extensive, only these four formulations have been selected for study. However, the nonerosive burning rate vs pressure data for many of the additional formulations have been utilized in order to determine the appropriate values of constants required as input into the PEM.

As is the case with many theoretical combustion models employed within the research community today, this model requires as input various propellant formulation properties, surface decomposition/gasification parameters, and gas-phase kinetic constants as well as various thermodynamic and transport property values. For this series of AP-based propellant formulations, the nonerosive burning rate vs pressure data have been used to determine, within accepted limits, the best values of only four gas-phase kinetic constants associated with the AP monopropellant flame and the primary flame. All other input parameters have been obtained from the literature as deemed appropriate for this type of composite solid propellant. Figure 5 presents the experimental, nonerosive burning rate vs pressure data for each of the four propellant formulations considered. The lines designated by their respective formulation represent the theoretical predictions obtained by the PEM. The PEM's predictions are excellent over the pressure range considered for all but the 200  $\mu\text{m}$  propellant formulation, 5051. It will be shown in the next section that under zero cross-flow conditions, the theoretical burning rate decreases dramatically with increasing oxidizer particle size for oxidizer diameters greater than say 50  $\mu\text{m}$ . This dramatic drop-off has not been

exhibited by the experimental data presented for formulation 5051.

The solid line in Fig. 5, that is, the theoretical rate vs pressure results for formulation 4525, will be treated as a baseline condition in the comparisons to be conducted. As can be observed in this figure, decreasing the oxidizer particle size at a constant solids loading greatly increases the burning rate at a given pressure. Similarly, for identical oxidizer particle diameter formulations, an increase in the combustion flame temperature due to an increase in the solids loading results in a corresponding increase in the base, or zero cross-flow, burning rate. Therefore, the erosive burning results for formulations 4685 and 5542 will be compared to those obtained for the baseline formulation, 4525, in order to observe the sensitivity of erosive burning to the base, or zero cross-flow, burning rate of a propellant.

Figure 6 depicts both the experimental and theoretical erosive burning sensitivity to cross-flow velocity for the baseline propellant formulation, 4525. In this figure, the burning rate is presented as a function of combustion pressure for cross-flow velocities ranging 0-670 m/s in magnitude. The data points represent the experimental results reported by King,<sup>10</sup> whereas the lines correspond to the predicted erosive PEM results for the cross-flow velocities listed. From this figure, it is evident that the contribution to the total burning rate due to erosive burning can be substantial, especially for high cross-flow velocities at elevated pressures. The erosive PEM tends to underpredict the magnitude of the erosive burning rate at the lower values of cross-flow velocity while overpredicting at the higher values of cross-flow velocity. However, the proper trend of increased erosive burning sensitivity with increased cross flow and pressure is exhibited as is observed from the experimental data presented.

To observe the effect of cross-flow velocity and combustion pressure on the erosive burning sensitivity of composite solid propellant, Fig. 7 has been presented. In this figure, the erosive burning enhancement factor, defined as the ratio of the actual propellant burning rate to the base, or zero cross-flow, burning rate, is plotted vs cross-flow velocity for formulation 4525 at four separate values of pressure, 1, 2, 3, and 4 MPa. The experimental data given by King<sup>10</sup> for this propellant are also presented in the figure. This figure shows the existence of the threshold velocity, that is, a value of the cross-flow velocity above which burning rate enhancement occurs. Also from this figure, it is evident that the magnitude of this threshold velocity decreases with increasing pressure. Therefore, the first two experimental observations listed above have been predicted by the erosive PEM for the specified propellant formulation.

Figures 8 and 9 depict the erosive burning sensitivity to both cross-flow velocity and pressure for the 5  $\mu\text{m}$  oxidizer particle

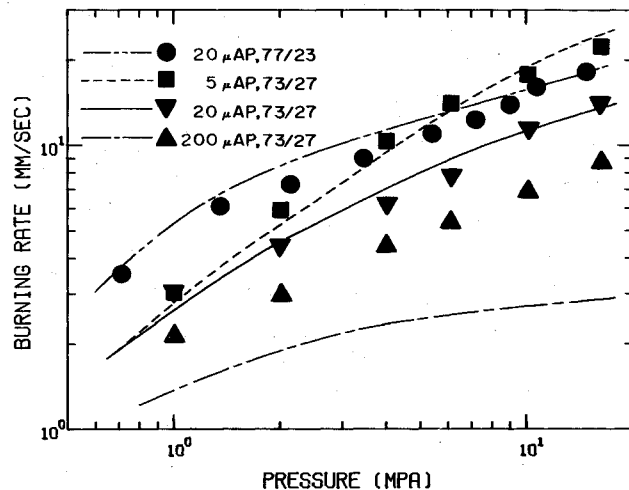


Fig. 5 Nonerosive burning rate data.

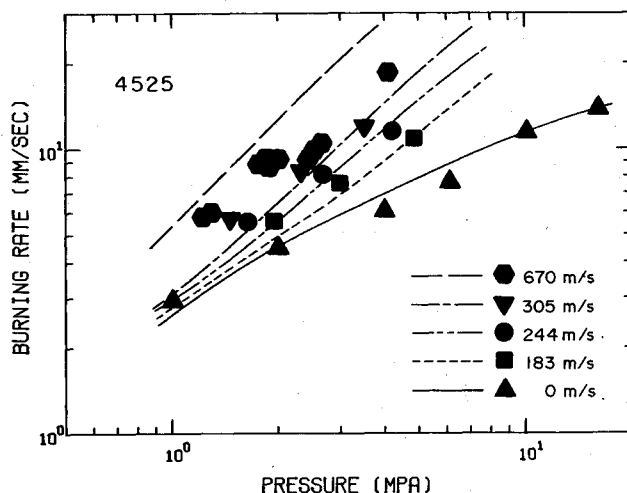


Fig. 6 Erosive burning rate data.

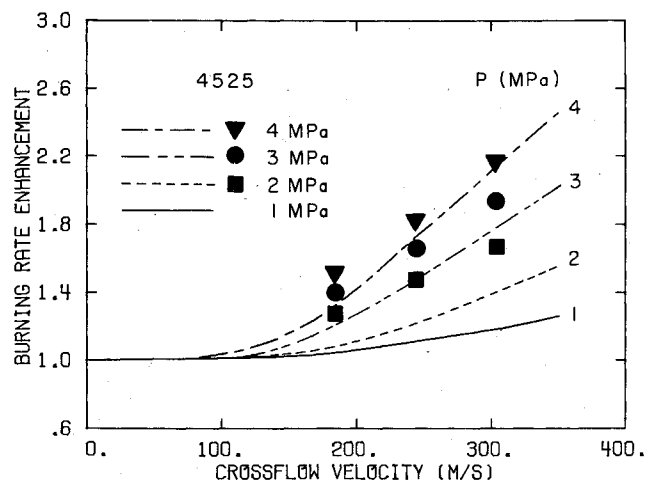


Fig. 7 Threshold velocity data.

diameter formulation, 4685, and the increased solids loading formulation, 5542, respectively. Both of these propellants have higher base, or zero cross-flow, burning rates than that exhibited by the baseline propellant formulation, 4525. In each of these two figures, both experimental data and corresponding theoretical predictions have been presented. From these two sets of results it is obvious that the erosive burning sensitivity of a propellant decreases with increasing base, or zero cross-flow, burning rate. Therefore, the erosive PEM has been shown to exhibit results consistent with the third experimentally observed trend listed above. More precisely, erosive burning sensitivity is shown to be greater for slower burning propellant formulations.

### Particle Size Effects

Selection of the oxidizer particle size can be an important parameter in the formulation of composite solid propellants. Previous theoretical works by the authors<sup>4,5,14</sup> have pointed out how the selection of the oxidizer particle size can greatly influence the value of steady-state combustion parameters such as burning rate, pressure exponent, and temperature sensitivity. In a similar manner, the erosive burning PEM has the capability of illustrating the effects of oxidizer particle size on the erosive burning rate.

The effect of oxidizer particle size on the calculated erosive burning rate is depicted in Fig. 10 where the burning rate for a series of unimodal, monodisperse "computer" propellants is plotted as a continuous function of oxidizer particle size for

several cross-flow velocities. To be consistent with the previous calculations, each "computer" propellant considered is a 73% solids AP/HTPB formulation and the erosive burning rate results are given for a pressure of 2 MPa and an initial solid-propellant temperature of 294 K. As before, the surface roughness is assumed to be equal to the oxidizer particle size, and only the boundary-layer displacement factor is included with the modified van Driest damping factor. The modified van Driest damping factor is assumed to be equal to unity.

It can be seen from this figure that erosive burning effects appear at lower values of mainstream cross-flow velocity for the propellants with larger oxidizer particle size. That is, erosive burning is encountered more readily in propellants with lower base, or zero cross-flow, burning rates. Also from this figure, it is evident that for any given erosive condition, i.e., cross-flow velocity, pressure, and initial temperature, a critical oxidizer particle size is exhibited below which erosive burning effects will not occur. Finally, this critical particle size decreases with increasing cross-flow velocity.

### Discussion of Results

Two questions may be asked regarding the erosive PEM's predictive capability. First, does the model predict the generally observed experimental trends, the presence of a threshold velocity, etc? Second, does the model predict quantitatively the erosive burning effect for a particular composite propellant formulation?

In response to the first question, this paper presented calculations with the erosive PEM demonstrating that the model has the capability of predicting all three of the experimental observed trends described above. One of the more predominant experimental observations is that, as the flow velocity across a burning propellant surface is increased, little effect on the burning rate is observed until the cross-flow velocity reaches a certain value, the threshold velocity. Figure 7 illustrates that the model does indeed predict a threshold velocity effect.

The threshold velocity effect is due to the interaction between blowing at the burning surface and the cross-flow-induced turbulent boundary layer. At low cross-flow velocities, the blowing parameter is very high. Consequently, the shear stress at the propellant surface is very low and the boundary layer in the flame zone region directly above the surface is effectively thinned or, in other words, the velocity profile is steepened. Thus, the contribution of turbulence to the transport property enhancement in the gas-phase reaction zone is rather small. As the cross-flow velocity is increased, a point is finally reached where the effect of turbulence is felt in the gas-phase reaction zone. Further increases in the cross-

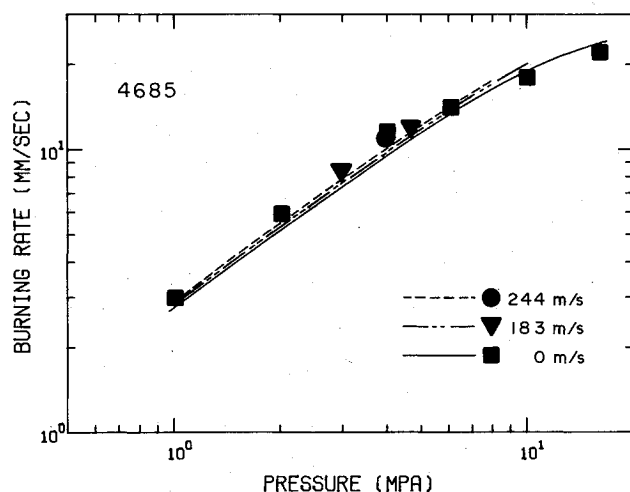


Fig. 8 Erosive burning rate data.

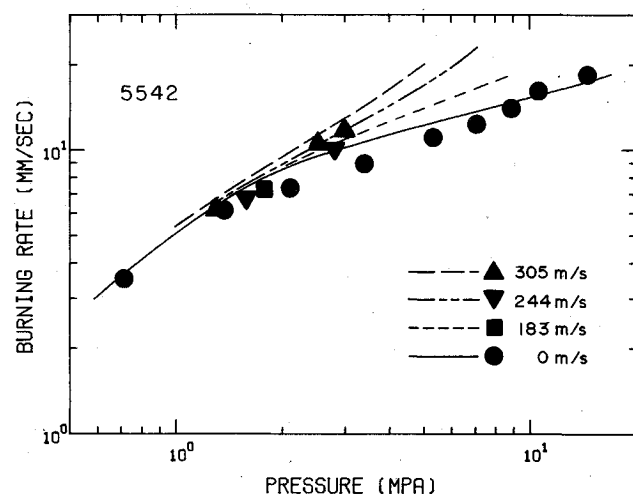


Fig. 9 Erosive burning rate data.

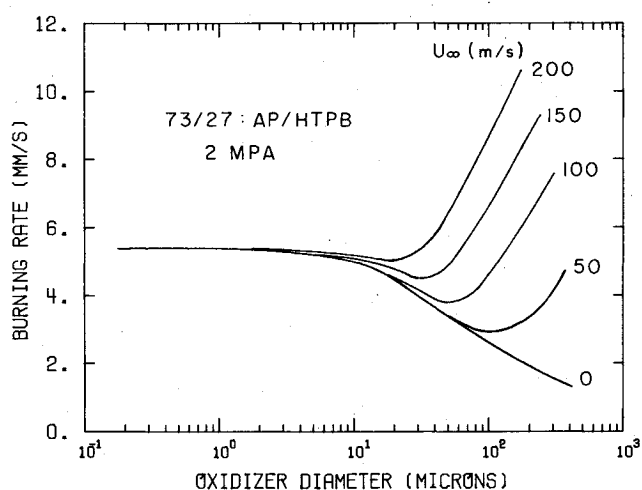


Fig. 10 Burning rate.



flow velocity result in increases in the transport property enhancement within the gas-phase reaction zone due to the increased level of turbulence in that region.

The dependency of threshold velocity on pressure as illustrated in Fig. 7 can also be explained in terms of the complex interaction between blowing at the propellant surface and the cross-flow-induced turbulent boundary layer. Calculations discussed previously show that a decrease in pressure causes a dramatic increase in the blowing parameter and a steepening in the velocity profile. This effect is primarily due to the reduction in gas-phase density with decreased pressure. Therefore, for the same value of cross-flow velocity, an increase in pressure will result in an increase in the transport property enhancement near the surface, thereby causing the threshold velocity to decrease with increasing pressure.

The effect of base, or zero cross-flow, burning rate on a propellant's erosive burning sensitivity can be explained by the effect of blowing on the turbulent boundary layer. For a given cross-flow velocity, the higher the burning rate, or blowing parameter, the less turbulence penetrates into the gas-phase reaction zone above the propellant surface. Therefore, the experimental observation that slower burning propellants are more sensitive to cross-flow velocity is also predicted by the erosive PEM.

In Fig. 6, King's<sup>10</sup> experimental data for propellant formulation 4525 have been included to assess the model's quantitative predictive capability of the erosive burning effect of a particular composite propellant. From the calculations presented it is evident that the results of the PEM coupled to an approximate turbulent boundary-layer analysis are in fair agreement with experiment. Most importantly though, the proper erosive burning trends have been exhibited as discussed above and presented in Figs. 7-9.

In addition to the above, the erosive PEM has been employed to determine the effect of oxidizer particle size on the erosive burning sensitivity for various cross-flow velocities. Figure 10 shows the effect of oxidizer particle diameter on the burning rate for a series of unimodal, monodisperse propellants. The burning rate for four values of cross-flow velocity, 50, 100, 150, and 200 m/s, is presented along with the nonerosive, zero cross-flow burning rate. From this figure it is evident that erosive burning sensitivity is considerably greater for the larger oxidizer particles. The reason that propellants with large oxidizer particles are the first to experience erosive burning is due to the fact that the flames above such particles are of sufficient height that they extend well into the boundary layer. As a result, the flame zones above the larger particles experience greater transport property enhancement due to increased turbulence levels present. As the cross-flow velocity is increased, the turbulence level increases closer to the burning surface, and the smaller oxidizer particles begin to burn erosively. The result is an enhanced burning rate for these particles.

The particle size effect can also be discussed in terms of the multiple flame structure situated above the oxidizer particles. The combustion of large oxidizer particles is normally dominated by the kinetically controlled AP monopropellant flame since the characteristic diffusion times are so large. However, as the mainstream cross-flow velocity is increased and turbulence finally extends into the final flame zone, the transport properties within the final flame are enhanced. This decreases the characteristic diffusion time and increases the heat transfer from the final flame to the propellant surface. The kinetically controlled AP flame, on the other hand, is driven away from the surface due to increased mass flow. Thus, as the cross-flow velocity is increased, the kinetically controlled AP flame becomes less dominant, and the final flame becomes more dominant. The increased erosive burning with increased oxidizer particle size can also, in part, be attributed to the increase in surface roughness and its effect on the boundary-layer characteristics discussed previously.

Finally, from Fig. 10 it is evident that for a given cross-flow velocity, there is a critical oxidizer particle diameter below which no erosive burning effect is experienced. The existence of a critical oxidizer particle diameter may be explained again on boundary-layer/turbulence level considerations. That is, a critical combination exists for the oxidizer particle size (flame structure) and the average transport property enhancement for which the burning rate enhancement is negligibly small. Increasing either the oxidizer particle size or the cross-flow velocity increases the burning rate enhancement. Thus, a critical oxidizer particle diameter exists for a given cross-flow velocity/pressure combination.

## Conclusions

In this paper, an erosive burning model which employs a statistical, steady-state combustion model, the petite ensemble model, coupled to an approximate transpired boundary-layer analysis has been presented. Erosive burning computational results utilizing this model agreed with traditionally observed experimental trends. That is, a threshold velocity is predicted that decreases with increasing pressure. Also, erosive burning sensitivity is calculated to be greater for slower burning propellants. In addition, the erosive PEM predicts that a critical oxidizer particle size exists below which erosive burning is not present and this critical oxidizer particle size decreases with increasing cross-flow velocity. These effects are all related to the flame structure in addition to the influence of transport property enhancement caused by the presence of a turbulent boundary layer above a transpiring propellant surface. The characteristics of the turbulent boundary layer have been shown to be strongly related to cross-flow velocity, burning rate, pressure, and surface roughness.

## Acknowledgments

This research has been sponsored by the Air Force Office of Scientific Research, Air Force Systems Command, USAF, under Grant AFOSR-77-3381. The United States Government is authorized to reproduce and distribute reprints for Governmental purposes notwithstanding any copyright notation hereon.

## References

- <sup>1</sup>Kuo, K. K. and Razdan, M.K., "Review of Erosive Burning of Solid Propellants," *Twelfth JANNAF Combustion Meeting*, CPIA Pub. 273, Vol. II, Dec. 1975, pp. 323-338.
- <sup>2</sup>King, M. K., "A Model of Erosive Burning of Composite Propellants," *Journal of Spacecraft and Rockets*, Vol. 15, May-June 1978, pp. 139-146.
- <sup>3</sup>Beddini, R. A., "Analysis of Injection-Induced Flows in Porous-Walled Ducts with Application to the Aerothermochemistry of Solid-Propellant Motors," Ph.D. Thesis, Rutgers University, New Brunswick, N.J., 1981.
- <sup>4</sup>Condon, J. A. and Osborn, J. R., "The Effect of Oxidizer Particle Size Distribution on the Steady and Nonsteady Combustion of Composite Propellants," AFRPL-TR-78-17, June 1978.
- <sup>5</sup>Renie, J. P., and Osborn, J. R., "Combustion Response Calculations for Composite Solid Propellants," AFRPL-TR-81-25, Dec. 1981.
- <sup>6</sup>Corner, J., "The Effects of Turbulence on Heterogeneous Reaction Rates," *Transactions of the Faraday Society*, Vol. 43, 1947, pp. 635-642.
- <sup>7</sup>Lengelle, G., "Model Describing the Erosive Combustion and Velocity Response of Composite Propellants," *AIAA Journal*, Vol. 13, March 1975, pp. 315-322.
- <sup>8</sup>Renie, J. P. and Osborn, J. R., "Pressure and Velocity Coupled Response of Composite Solid Propellants Based Upon a Small Perturbation Analysis," AIAA Paper 81-1556, July 1981.
- <sup>9</sup>Renie, J. P. and Osborn, J. R., "Erosive Burning," AIAA Paper 79-0165, Jan. 1979.
- <sup>10</sup>King, M. K., "A Model of the Effects of Pressure and Crossflow Velocity on Composite Propellant Burning Rate," AIAA Paper 79-1171, June 1979.



<sup>11</sup>Glick, R. L., "On Statistical Analysis of Composite Solid Propellant Combustion," *AIAA Journal*, Vol. 12, March 1974, pp. 384-385.

<sup>12</sup>Beckstead, M. W., Derr, R. L., and Price, C. F., "A Model of Composite Solid-Propellant Combustion Based on Multiple Flames," *AIAA Journal*, Vol. 8, Dec. 1970, pp. 2200-2207.

<sup>13</sup>Glick, R. L. and Condon, J. A., "Statistical Analysis of Polydisperse Heterogeneous Propellant Combustion: Steady State," *Thirteenth JANNAF Combustion Meeting*, CPIA Pub. 281, Vol. II, Dec. 1976, pp. 313-345.

<sup>14</sup>Renie, J. P., Condon, J. A., and Osborn, J. R., "Oxidizer Size Distribution Effects on Propellant Combustion," *AIAA Journal*, Vol. 17, Aug. 1979, pp. 877-883.

<sup>15</sup>Rubensin, M. W., "An Analytical Estimation of Transpiration Cooling on the Heat Transfer and Skin-Friction Characteristics of a Compressible Turbulent Boundary Layer," NACA TN-3341, Dec. 1954.

<sup>16</sup>Schlichting, H., *Boundary Layer Theory*, 4th ed., McGraw-Hill Book Co., New York, 1960.

<sup>17</sup>Cebeci, T. and Chang, K. C., "Calculation of Incompressible Rough-Wall Boundary-Layer Flows," *AIAA Journal*, Vol. 16, July 1978, pp. 730-735.

<sup>18</sup>Kays, W. M. and Moffat, R. J., "The Behavior of Transpired Turbulent Boundary Layers," Thermosciences Division, Dept. of Mechanical Engineering, Stanford University, Stanford, Calif., Rept. HMT-20, April 1975.

<sup>19</sup>van Driest, E. R., "On Turbulent Flow Near a Wall," *Journal of the Aeronautical Sciences*, Vol. 23, Nov. 1956, pp. 1007-1011.

<sup>20</sup>Landis, R. B. and Mills, A. F., "The Calculation of Turbulent Boundary Layers with Foreign Gas Injection," *International Journal of Heat and Mass Transfer*, Vol. 15, Oct. 1972, pp. 1905-1932.

<sup>21</sup>Kutateladze, S. S. and Leontev, A. I., *Turbulent Boundary Layers in Compressible Gases*, translated by D. B. Spalding, Academic Press, New York, 1964.

<sup>22</sup>Schetz, J. A. and Nerney, B., "Turbulent Boundary Layer with Injection and Surface Roughness," *AIAA Journal*, Vol. 15, Sept. 1977, pp. 1288-1294.

<sup>23</sup>Mickley, H. S. and Davis, R. S., "Momentum Transfer for Flow over a Flat Plate with Blowing," NACA TN-4017, Nov. 1957.

## *From the AIAA Progress in Astronautics and Aeronautics Series . . .*

### **TRANSONIC AERODYNAMICS—v. 81**

*Edited by David Nixon, Nielsen Engineering & Research, Inc.*

Forty years ago in the early 1940s the advent of high-performance military aircraft that could reach transonic speeds in a dive led to a concentration of research effort, experimental and theoretical, in transonic flow. For a variety of reasons, fundamental progress was slow until the availability of large computers in the late 1960s initiated the present resurgence of interest in the topic. Since that time, prediction methods have developed rapidly and, together with the impetus given by the fuel shortage and the high cost of fuel to the evolution of energy-efficient aircraft, have led to major advances in the understanding of the physical nature of transonic flow. In spite of this growth in knowledge, no book has appeared that treats the advances of the past decade, even in the limited field of steady-state flows. A major feature of the present book is the balance in presentation between theory and numerical analyses on the one hand and the case studies of application to practical aerodynamic design problems in the aviation industry on the other.

696 pp., 6 × 9, illus., \$30.00 Mem., \$55.00 List

TO ORDER WRITE: Publications Order Dept., AIAA, 1633 Broadway, New York, N.Y. 10019